Universitat de Girona

Facultat de Ciències

Memòria del Treball Final de Grau

New ruthenium complexes containing N- or/and S-donor type of ligands as catalysts for nitrile hydration

---

Estudiant: Patrícia Lopes Villena Grau en Química

Correu electrònic: plopesvillena@gmail.com

Tutor: Mª Isabel Romero

Vistiplau tutor:

Nom del tutor: Mª Isabel Romero

Correu(s) electrònic(s): marisa.romero@udg.edu

Data de dipòsit de la memòria a secretaria de coordinació: 23-07-2015

AGRAÏMENTS

A la Doctora Marisa Romero, tutora del treball de fi de grau, per la seva exigència, l'orientació i la confiança d'acompanyar-me durant la trajectòria del projecte. Gràcies al grup de recerca que ha col·laborat en el meu projecte, per tota l'ajuda i la paciència que m'heu dedicat, en especial a Lorena Capdevila pel seu constant suport. A les meves amistats i les meves companyes de la universitat que m'han acompanyat sempre i han fet més amè el recorregut. També vull esmentar com no, la família: els meus pares Narcís i Tere amb el seu estímul, recolzament i estima inqüestionable; i al meu germà Narcís, un pilar indispensable.

RESUM

En aquests treball de final de grau es presenta la síntesi i caracterització de nous complexos de ruteni amb la idea d'estudiar la seva química de coordinació, així com l'activitat catalítica dels complexos sintetitzats en la hidròlisis de nitrils.

Es descriu la síntesi i caracterització espectroscòpica i redox dels nous complexos de ruteni, Ru-Cl i Ru-DMSO, que contenen el lligand neutre 1,4,7–tritiaciclononà (9S3) i el lligand no simètric bidentat 2-(3-pirazolil)piridina (pypz-H). En primer lloc, s'ha dut a terme la síntesi dels complexos $[Ru^{II}Cl_2(DMSO)_4]$ **[1]** i $[Ru^{II}Cl_2(9S3)(DMSO)]$ **[2]**, on ambdós s'utilitzen com a productes de partida per a l'obtenció del cloro complex $[Ru^{II}Cl(pypz\text{-}H)(9S3)]Cl$ **[3]**. Així mateix el complex $[Ru^{II}(pypz\text{-}H)(9S3)(DMSO)](PF_6)_2$ **[4]** també ha estat sintetitzat a partir del complex **[3]** mitjançant la substitució d'un lligand cloro (Cl) per un lligand dimetil sulfòxid (DMSO).

La caracterització dels complexos s'ha dut a terme en estat sòlid mitjançant anàlisi elemental i espectroscòpia infraroja (IR), i en dissolució mitjançant tècniques espectroscòpiques com ressonància magnètica nuclear (NMR), ultraviolat visible (UV-Vis) i voltametria cíclica (CV).

S'ha estudiat el comportament químic dels complexos Ru-Cl **[3]** i Ru-DMSO **[4]** en aigua mitjançant espectroscòpia UV-Vis. S'ha observat en tots dos casos la substitució dels lligands cloro i DMSO pel lligand aqua i conseqüentment, s'ha estudiat la cinètica d'aquació dels dos complexos. També s'han estudiat les propietats redox en funció del pH del aqua complex de ruteni resultant, mitjançant un diagrama de Pourbaix.

Finalment s'ha analitzat la capacitat catalítica d'aquests complexos en la reacció de hidròlisis de nitrils utilitzant aigua com a dissolvent i els nitrils benzonitril i acrilonitril com a substrats. Els complexos mostren valors de conversió moderats i excel·lents valors de selectivitats per les corresponents amides.

L'estructura dels nous complexos sintetitzats es mostra a continuació:

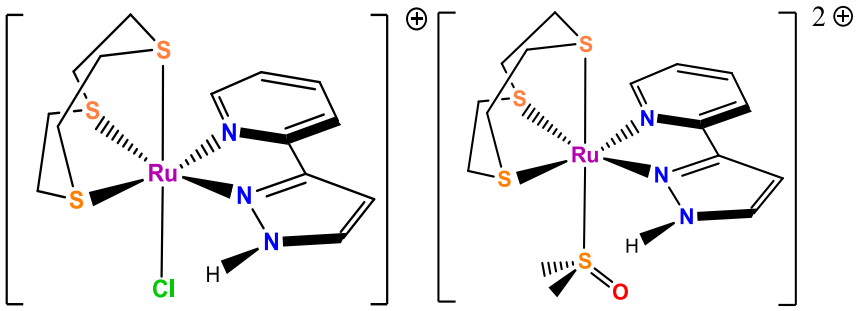

RESUMEN

En este trabajo de final de grado se presenta la síntesis y caracterización de nuevos complejos de rutenio con la idea de estudiar su química de coordinación así como su actividad catalítica en la hidrólisis de nitrilos.

Se describe la síntesis y caracterización espectroscópica y redox de los nuevos complejos de rutenio, Ru-Cl y Ru-DMSO, que contienen el ligando neutro 1,4,7–tritiaciclononano (9S3) y el ligando no simétrico bidentado 2-(3-pirazolil)piridina (pypz-H). En primer lugar, se ha llevado a cabo la síntesis de los complejos $[Ru^{II}Cl_2(DMSO)_4]$ **[1]** y $[Ru^{II}Cl_2(9S3)(DMSO)]$ **[2]**, donde ambos se utilizan como productos de partida para la obtención del cloro complejo $[Ru^{II}Cl(pypz\text{-}H)(9S3)]Cl$ **[3]**. Asimismo el complejo $[Ru^{II}(9S3)(pypz)(DMSO)](PF_6)_2$ **[4]** también ha sido sintetizado a partir del complejo **[3]** mediante la sustitución de un ligando cloro (Cl) por un ligando dimetil sulfóxido (DMSO).

La caracterización de los complejos se ha llevado a cabo en estado sólido mediante análisis elemental y espectroscopia infrarroja (IR), y en disolución mediante técnicas espectroscópicas como resonancia magnética nuclear (NMR), ultravioleta visible (UV-Vis) y voltametría cíclica (CV).

Se ha estudiado el comportamiento químico de los complejos Ru-Cl **[3]** y Ru-DMSO **[4]** en agua a través de UV-Vis. Se ha observado en ambos casos la substitución de los ligandos cloro y DMSO por el ligando aqua y consecuentemente se ha estudiado la cinética de aquación de los dos complejos. También se ha estudiado las propiedades redox en función del pH del aqua complejo de rutenio resultante, mediante un diagrama de Pourbaix.

Finalmente se ha analizado la capacidad catalítica de los complejos en la reacción de hidrólisis de nitrilos utilizando agua como disolvente y los nitrilos benzonitrilo y acrilonitrilo como sustratos. Los complejos muestran moderados valores de conversión y excelentes valores de selectividad por las correspondientes amidas.

La estructura de los nuevos complejos sintetizados se muestra a continuación:

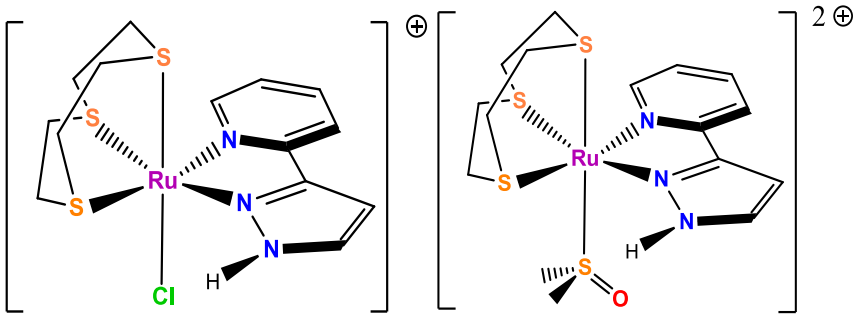

ABSTRACT

In this work, we present the synthesis and characterization of new ruthenium complexes with the idea of studying their coordination chemistry, as well as their performance in nitrile hydration reactions.

We describe the synthesis and the spectroscopy and redox characterization of new ruthenium compounds, Ru-Cl and Ru-DMSO. These complexes contain the neutral 1,4,7–trithiacyclononane (9S3) and the non-symmetric didentate 2-(3-pyrazolyl)pyridine (pypz-H) ligands. Firstly, we have synthesized the complex $[Ru^{II}Cl_2(DMSO)_4]$ **[1]** and $[Ru^{II}Cl_2(9S3)(DMSO)]$ **[2]**. Both have been used as starting material for the synthesis of chlorido complex $[Ru^{II}Cl(pypz\text{-}H)(9S3)]Cl$ **[3]**. Moreover, complex $[Ru^{II}(9S3)(pypz)(DMSO)](PF_6)_2$ **[4]** have been also synthesized from complex **[3]** by replacing chlorido ligand (Cl) by dimethyl sulfoxide ligand (DMSO).

The new complexes have been characterized in solid state through elemental analysis and infrared spectroscopy (IR) and in solution through spectroscopic techniques as nuclear magnetic resonance (NMR), ultraviolet visible (UV-Vis) and cyclic voltammetry (CV).

The chemical behavior in aqueous solution has been tested for the two complexes Ru-Cl **[3]** and Ru-DMSO **[4]** through UV-Vis. In both cases, substitution of chlorido and DMSO ligands for aqua ligand has been observed and consequently we have studied the kinetics of aquation for both complexes. We also have studied the pH-dependent redox properties for the resulting aqua ruthenium complex through a Pourbaix diagram.

Finally, the catalytic activity of the complexes in nitrile hydration reaction is evaluated in water using nitriles like benzonitrile and acrylonitrile as substrates. All compounds have shown moderate conversions and high selectivities values towards the corresponding amides.

The structure of the new complexes used in this work is shown below:

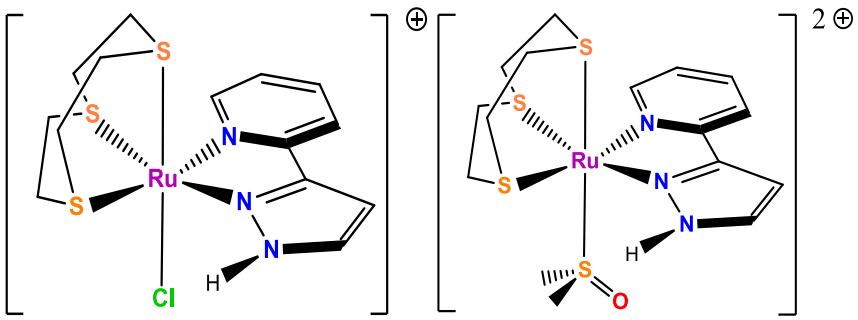

GLOSSARY OF TERMS AND ABBREVIATIONS

9S3	1,4,7 – trithiacyclononane
A	Absorbance
A∞	Absorbance at infinite time
A_t	Absorbance at determinate time
Anal. Found (Calc.)	Analysis found (analysis calculated)
Bpp	Bis(2-pyridyl)pyrazole
$C_{10}H_{12}N_2O$	3-dimethylamino-1-(pyridine-2-yl)prop-2-en-1-one
ca.	Approximately
Cl	Chlorido
Cl-tpy	4-chloro-2,2';6',2''-terpyridine
COSY	Correlation spectroscopy
CV	Cyclic voltammetry
d	Doblet
dach	1,2-diaminocyclohexane
DMSO	Dimethyl sulfoxide
ε	Extinction coefficient
E	Potential
$E_{1/2}$	Half-wave potential
E_{pa}	Anodic pic potential
E_{pc}	Cathodic pic potential
ESI-MS	Electrospray ionization mass spectrometry
GC	Gas chromatography
h	Hours
HMBC	Heteronuclear multiple bond correlation
HSQC	Heteronuclear single-quantum correlation
IR	Infrared
J	Coupling constant
M	Metal
m	Multiplet
MLCT	Metal to ligand charge transfer
MeOH	Methanol
m/z	Mass-to-charge ratio
NMR	Nuclear magnetic resonance
NOESY	Nuclear Overhauser effect spectroscopy
PCET	Proton-coupled-electron transfer
ppm	Parts per million
ptt	1-(2-picolyl)-4-phenyl-1H-1,2,3-triazole
pypz-H	2-(3-pyrazolyl)pyridine
S	Sulfur

s	Singlet
sel.	Selectivity
Ru	Ruthenium
T	Temperature
t	Triplet
TBAH	Tetra(n-butyl)ammonium hexafluorophosphate
tpy	2,2';6',2''-terpyridine
UV-Vis	Ultraviolet-visible spectroscopy
vs	Versus
λ	Wavelength

Table of contents

CHAPTER 1. INTRODUCTION

1.1 Ruthenium complexes properties

Ruthenium is a metal situated in the d group of the periodic table. The electronic configuration of ruthenium ([Kr] $4d^7\,5s^1$) makes this metal, together with osmium, unique among most of the elements in displaying the widest range of oxidation states in their complexes. The oxidation state of ruthenium takes place from -2 as in $[Ru(CO)_2]^{2+}$ (d^0) to +8 as in RuO_4 (d^{10}). The synthetic versatility and the kinetic stability of ruthenium complexes in different oxidation states make these complexes particularly interesting. Other characteristics of ruthenium's coordination compounds are their high electron transfer capacity,[1] a robust character of their coordination sphere, their redox-active capacity, their easily available high oxidation states and their applications as redox reagents in many different chemical reactions.

Ruthenium complexes have experienced a large boost in the fields of catalysis,[2] photochemistry and photophysics,[3] and more recently in supramolecular[4] and bio-inorganic chemistry.[5]

The properties of ruthenium complexes are certainly correlated with the nature of the ligands coordinated to the central metal ion. Ruthenium complexes with N-donor ligands are studied due to their spectroscopic, photophysical and electrochemical properties.[6] On the other hand, ruthenium complexes with π-conjugate ligands or systems that enable electronic delocalization have shown specific properties in nonlinear optics, magnetism, molecular sensors and liquid crystals.[7] Moreover, sulfoxide complexes have been extensively studied due to their relevant usefulness in chemotherapy.[8]

1.2 Applications of ruthenium complexes with N or/and S-donor ligands

In recent years, the study on ruthenium complexes with N-donor ligands have received much attention owing to their interesting uses in diverse areas such as photo sensitizers for photochemical conversion of solar energy,[9] molecular electronic divides[10] and photoactive DNA cleavage agents for therapeutic purposes.[11]

Chemistry of transition metal complexes with S-donor ligands has been increased since when the first articles were published in the sixties. These complexes are really useful as starting material in synthesis of new organometallic and coordination compounds,[12] they are also applied in catalytic processes[13] and as antitumor compounds.[14]

Ruthenium complexes containing the tridentate sulfur macrocycle 1,4,7-trithiacyclonane have been studied as potential compounds with antitumor activity.[15] Another application of ruthenium complexes with 9S3 ligands is to be used in self-assembly reactions.[16]

1.2.1. Ruthenium complexes with DMSO ligand

After the first transition metal complexes with sulfoxide ligands were reported in the 1960s,[17] its chemistry has been quickly expanded. The interest of these compounds relays on their utility in medicinal chemistry as antitumor compounds[18] and antimetastatic agents.[19]

The properties of this kind of complexes are closely associated with the nature of the metal-sulfoxide bond. Ruthenium complexes have the capacity to been coordinate for both oxygen and sulfur atoms illustrating linkage isomerism. For this reason, the understanding of the factors which affects the bond mode is important for the study of these complexes.

DMSO ligand coordinates through the sulfur atom with elements of the second and third transition series, such as Ru(II) d^6 low spin configuration, and with some metals from VI and VII group. The metal-oxygen bond is common in tough metals like Ru(III). According to the acid-base theory of Pearson, diffuse orbitals of soft metal ions overlap better with other orbitals also widespread like S donors. The M-S bond is favored if it exist π-retrodonation from metal orbitals to DMSO orbitals, as this ligand has π-acceptor properties. This happen to Ru(II), which stabilizes the Ru-S bond yielding π-electron density to the empty orbitals of the DMSO ligand. When it has an oxidation of Ru(II) to Ru(III), as it decreases the ability of π-retrodonation from metal orbitals to DMSO orbital, the distance between Ru-S increases. This trend has been confirmed in numerous complexes Ru-DMSO.[20]

Since the introduction of $[Ru(Cl)_2(DMSO)_4]$ by Wilkinson *et al.* in 1973[21] a huge number of ruthenium compounds containing DMSO ligands combined with a variety of auxiliary ligands have been described. DMSO ligand is classified as a versatile molecule for the development of Ru based initiators for a variety of catalytic reactions because of its ambidentate behavior. Some of these catalytic reactions such as hydrogenation,[22] oxidation of aliphatic ethers to esters[23] or isomerization of alcohols[24] are important for the industry.

1.3 Ruthenium polypyridyl aqua complexes

Extensive coordination chemistry about hexacoordinated complexes containing polypyridyl ligands has been reported, due to these ligands stability against oxidation and their great coordinative capacity, increased by their quelating effect. These properties give a great stability to the formed complex.

The redox properties of these complexes become especially interesting when an aqua ligand is directly bound to the metal center. In this case, a proton-coupled-electron transfer (PCET) is possible, making the high oxidation states fairly accessible.[25]

The successive oxidation from Ru(II) to Ru(IV) are accompanied by a sequential loss of protons favored by the enhanced acidity of the bonded aqua ligand (*Scheme 1*). Therefore, the initial Ru^{II}-OH_2 is oxidized to Ru^{IV}=O, passing through a Ru^{III}-OH species.

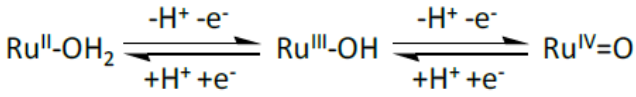

Scheme 1. PCET oxidation process characteristic of Ru-aqua complexes.

As a consequence of this behavior, the redox potentials of the aqua complexes are directly correlated with the pH of the medium in such a way that, if pH increases, the Ru(III/II) and Ru(IV/III) couples are shifted to lower potentials. The Nernst equation (*Equation 1*) correlates pH with redox potential in such a way that, for a monoprotic and monoelectronic transfer, the redox potential diminishes in 59 mV by every pH unit increased.

$$E_{1/2} = E^{o}_{1/2} - 0.059\ (m/n)\ pH \qquad (1)$$

$E_{1/2}$: half wave redox potential at a given pH
$E^{o}_{1/2}$: half wave redox potential at standard conditions
m: number of transferred protons
n: number of transferred electrons

Equation 1. Relation between potential and pH in the Nernst equation.

The graphical representation of this pH dependence in front of the redox potential is known as Pourbaix diagram. This diagram combines the redox equilibria with the acid/base equilibria of all the thermodynamically stable species involved and represents the dependence of the half wave redox potential, $E_{1/2}$, with respect to the complete pH range.

1.4 Ruthenium in catalysis

Ruthenium complexes can catalyze a variety of reactions. Our work will be focused on the nitrile hydration process.

1.4.1. Nitrile hydration reactions

The hydration of nitriles allows us to generate the corresponding amides. The amide bond is one of the most important functional groups in contemporary chemistry since amides not only constitute versatile building blocks in synthetic organic chemistry, but also exhibit a wide range of industrial applications and pharmacological interest.[26]

In the hydrolysis reaction of nitriles we have an acid/base[27] reaction with two steps: first a nucleophilic addition to produce an amide, and then a nucleophilic substitution to produce ammonium salt or carboxylic acid (*Scheme 2*).

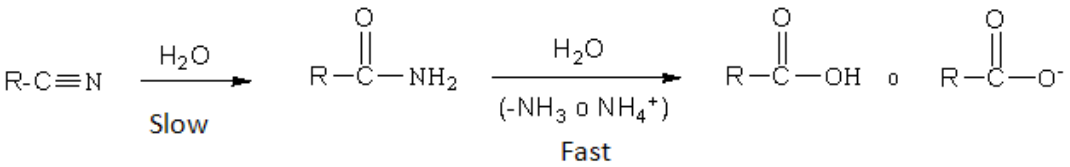

Scheme 2. The nitrile hydration and amide hydrolysis reactions.

Amides have been synthesized by the hydration of nitriles using strong acids and bases as catalyst. In addition, amides are commonly prepared by the reaction of activated carboxylic acid derivatives (acid chloridos, anhydrides and esters) with amines including ammonia or by direct union of the acids with the amines assisted by coupling reagents, such as carbodiimides or ^{1}H-benzotriazole derivatives.[28] However, these methods suffer from a low atom economy and under these conditions we generate different subproducts such as carboxylic acids, making their environmental profile unfavorable. Moreover, many sensitive functional groups do not endure hard conditions, which consequently decrease the selectivity of the reaction.

1.4.2. Nitrile hydration catalyzed by ruthenium

At the beginning, this reaction use to take place without metallic ions either acidic or basic conditions. However, this methodology is not efficient enough because most part of the amide product become to derivate acid. Extreme acidity and basicity can be avoided by using transition-metal complexes.

The participation of metal ions in the hydrolysis reaction of nitriles avoids the formation of by-products, salts and polymers. Also increase the rate velocity of nitriles hydrolysis obtaining the amide derivates. The application of a ruthenium complex to promote the selective hydration of nitriles to primary amides was described for the first time by Taube and co-workers in the 1970's.[29] It was not until 1992 that the first truly catalytic system could be developed by Murahashi and co-workers employing the ruthenium dihydride complex $[RuH_2(PPh_3)_4]$ as catalyst.[30]

A reaction pathway involving the intermolecular nucleophilic addition of water to the coordinated nitrile, to give an iminolate complex, was proposed (*Scheme 3*). Reductive elimination, isomerization of the iminol to the amide and subsequent dissociation generates the catalytically active ruthenium species.[31]

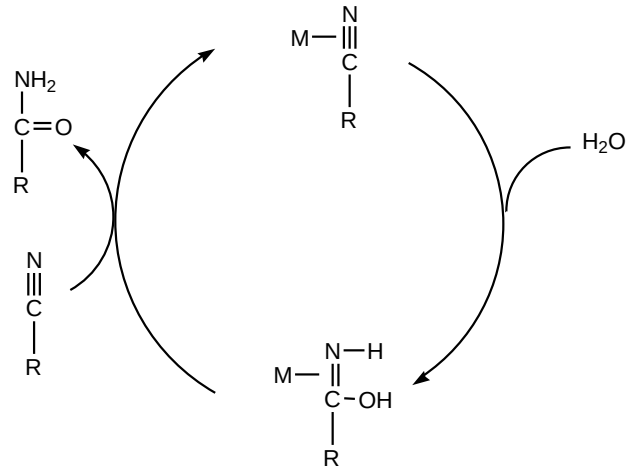

Scheme 3. Catalytic cycle of nitrile to amide.

A variety of transition-metal complexes have been investigated, Murahashi's ruthenium dihydride $[RuH_2(PPh3)_4]$[32] or Parkins's platinum hydride $PtH(PMe_2OH)\{(PMe_2O)_2H\}]$,[33] showing remarkable activities and selectivity's under mild conditions though in all cases operating in organic media in the presence of only small amounts of water. Recently, the group has published the first ruthenium complexes containing pyrazolic and DMSO type of ligands for applications in the hydrolysis of nitriles showing good conversion and excellent selectivity values. To the best of our knowledge, no report of Ru(II) complexes containing the 9S3 ligand together with pyrazolic ligands have been studied as catalysts in the nitrile hydration processes.

CHAPTER 2. OBJECTIVES

The aims of this work are the ones following:

1. To learn the techniques of synthesis and spectroscopic and electrochemical characterization, which are characteristic of a research laboratory.

2. The synthesis of a set of new ruthenium (II) complexes containing the S-tridentate 1,4,7-trithiacyclononane (9S3) ligand together with the bidentate 2-(3-pyrazolyl)pyridine (pypz-H), and the monodentate chlorido (Cl) or dimethyl sulfoxide (DMSO) ligands. The ligands used in this work are the ones following in the *Figure 1*.

Figure 1. Plot and labelling schemes for ligands used in this work: pypz-H, 9S3 and DMSO.

3. The spectroscopic and electrochemical characterization of the complexes synthesized.

4. The study of the chemical behavior in aqua solution and the kinetic of aquation of ruthenium (II) complexes, Ru-Cl and Ru-DMSO.

5. The evaluation of the previously synthesized complexes in catalytic nitrile hydration reaction in water medium.

CHAPTER 3. EXPERIMENTAL SECTION

3.1 Instrumentation and measurements

Elemental analyses

Elemental analyses were performed using a CHNS-O Elemental Analyser EA-1108 from Fisons. Monochromatic irradiations were carried out by using a 80 W lamp source from Phillips on complex solutions, typically 1mM.

UV-VIS

UV-VIS spectroscopy was performed on a Cary 50 Scan (Varian) UV-Vis spectrophotometer with 1 cm quartz cells.

Cyclic voltammetric

Cyclic voltammetric experiments were performed in an IJ-Cambria IH-660 potentiostat using a three electrode on one compartment cell. The working electrode potential is ramped linearly versus time; in this case glassy carbon electrode (3 mm diameter) from BAS was used as working electrode. Platinum wire was used as auxiliary electrode. Finally, Ag/AgCl was used as the reference electrode. The voltammetry was recorded using acetonitrile, dichloromethane or methanol solutions using TBAH as supporting electrolyte to yield a 0.1M ionic strength solution.

All half-wave potential values reported in this work were estimated from cyclic voltammetric experiments as the average of the oxidative and reductive peak potentials:

$$E_{1/2} = \frac{(E_{pa} + E_{pc})}{2} \quad (2)$$

IR

IR spectra were recorded using an Agilent Cary 630 FTIR Spectrometer.

^{1}H-NMR

The ^{1}H-NMR spectroscopies were performed on a Bruker DPX 400 and 300 MHz. Samples were run in different deutered solvents indicated in each case. The chemical shifts (δ) are given in units (ppm) using as reference tetramethylsilane (TMS).

Gas chromatography

Gas chromatography experiments were performed by capillary GC, using a GC-2010 Gas Chromatograph from Shimadzu, equipped with a Astec CHIRALDEX G-TA Column (30 m x 0.25 mm diameter) incorporating a FID detector. All the product analyses in the catalytic experiments were performed by means of GC using 0.1M biphenyl in $CHCl_3$ as internal standard.

3.2 Preparations

$[Ru^{II}Cl_2(DMSO)_4]$ **[1]**,[34] $[Ru^{II}Cl_2(9S3)(DMSO)]$ **[2]**[35] and $[Ru^{II}Cl_2(pypz\text{-}H)(DMSO)_2]$ **[1']**[36] complexes and the 2-(3-pyrazolyl)pyridine (pypz-H)[37] ligand were prepared according to literature procedures. All synthetic experiments were performed in the absence of light. 9S3 ligand and $C_{10}H_{12}N_2O$ (α,β-unsaturated ketone) were supplied by Aldrich and $RuCl_3 \cdot 2.38H_2O$ by Johnson Matthey.

2-(3-pyrazolyl)pyridine (pypz-H). A 2.022 g (10.9 mmol) sample of $C_{10}H_{12}N_2O$ (commercial ketone) in 20 mL of absolute ethanol was added to 0.70 ml of hydrazine. The reaction mixture was refluxed for 1 hour. A solid precipitate appears after cooling to room temperature and reducing the volume. The brown precipitate was filtered off and washed with diethyl ether and vacuum dried. Yield: 1.5 g (93%). Anal. Found (Calc.) for $C_8H_7N_3$: C, 66.11 (66.19); H, 4.77 (4.86); N, 28.84 (28.95). ^{1}H NMR (400 MHz, $CDCl_3$): δ = 6.79 (d, $^3J_{H,H}$ = 4 Hz, 1H, H7), 7.24 (t, $^3J_{H,H}$ = 8 Hz, 1H, H2), 7.65 (d, $^3J_{H,H}$ = 4 Hz, 1H, H8), 7.74 (t, $^3J_{H,H}$ = 8 Hz, 1H, H3), 7.75 (d, $^3J_{H,H}$ = 8 Hz, 1H, H4), 8.61 (d, $^3J_{H,H}$ = 8 Hz, 1H, H1) ppm.

$[Ru^{II}Cl_2(DMSO)_4]$ [1]. A 1.013 g (1.609 mmol) sample of $RuCl_3 \cdot 2.38H_2O$ were refluxed in 5 mL of DMSO for 10 min at 170°C. After cooling the mixture to room temperature, 10 mL of acetone were added. A yellow precipitate appeared, which was filtered and washed with acetone and ether and vacuum dried. Yield: 0.368 g (47%). Anal. Found (Calc.) for $C_8H_{24}Cl_2O_4RuS_4$: C, 19.79 (19.83); H, 4.81 (4.99). E_{pa} (CH_3CN + 0.1M TBAH): 1.15 V vs Ag/AgCl.

$[Ru^{II}Cl_2(9S3)(DMSO)]$ [2]. A 0.559 g (1.153 mmol) sample of $[Ru^{II}Cl_2(DMSO)_4]$ **[1]** were added to 0.214 g (1.153 mmol) of ligand 9S3 in 15 mL of ethanol. The light-protected solution was refluxed for 90 min at 80°C. After this time, the mixture was allowed to cool to room temperature and the volume was reduced. A yellow-orange precipitate was formed and collected on a frit, washed with ether and vacuum dried. Yield: 0.433 g (87%). Anal. Found (Calc.) for $C_8H_{18}Cl_2ORuS_4$: C, 22.75 (22.32); H, 3.92 (4.21). $E_{1/2}$ (CH_3CN + 0.1M TBAH): 0.98 V vs Ag/AgCl. UV-vis (CH_2Cl_2, 0.1 mM) [λ_{max} nm (ε, cm^{-1} M^{-1})]: 357 (3068), 426 (1555).

[Ru^{II}Cl(pypz-H)(9S3)]Cl [3]. In order to obtain the complex **[3]**, we have followed two synthetic strategies.

Strategy I

A 0.05 g (0.116 mmol) sample of [$Ru^{II}Cl_2$(9S3)(DMSO)] **[2]** were added to 0.022 g (0.152 mmol) of pypz-H in 10 mL of ethanol. The reaction mixture was refluxed for 21 h. During this time an orange solution was obtained. The volume of the resulting solution was reduced until the formation of an orange solid precipitate. The solid was washed with diethyl ether and vacuum dried. Yield: 0.031 g (60%). Anal. Found (Calc.) for $C_{14}H_{19}Cl_2N_3RuS_3$: C, 32.84 (32.95); H, 3.76 (3.82); N, 8.05 (8.25). ^{1}H NMR (400 MHz, MeOH(d)): δ = 2.48-3.04 (m, 12 H, CH_2 9S3), 7.24 (d, $^3J_{H,H}$ = 4 Hz, 1H, H7), 7.51 (t, $^3J_{H,H}$ = 8 Hz, 1H, H2), 8.02 (d, $^3J_{H,H}$ = 4 Hz, 1H, H8), 8.09 (t, $^3J_{H,H}$ = 8 Hz, 1H, H3), 8.19 (d, $^3J_{H,H}$ = 8 Hz, 1H, H4), 8.99 (d, $^3J_{H,H}$ = 8 Hz, 1H, H1) ppm. ^{13}C NMR (400 MHz, MeOH(d)): δ = 153.6 (C5), 152.7 (C1), 151.8 (C6), 138.0 (C3), 133.3 (C8), 124.7 (C2), 121.9 (C4), 104.21 (C7), 34.6 (CH_2 9S3), 34.2 (CH_2 9S3), 32.7 (CH_2 9S3), 32.4 (CH_2 9S3), 31.5 (CH_2 9S3), 30.6 (CH_2 9S3) ppm. IR ($\nu_{max,}$ cm^{-1}): 3336, 3059, 2653, 1437, 1370, 760. $E_{1/2}$(CH_3CN + 0.1M TBAH): 1.17 V vs Ag/AgCl. UV/Vis (H_2O, 0.1 mM) [λ_{max} nm (ε, cm^{-1} M^{-1})]: 270 (18098), 297 (7148), 355 (5390), 395 (4443). ESI-MS (m/z): 462 $[M\text{-}Cl]^+$.

Strategy II

A 0.006 g (0.011 mmol) sample of [$Ru^{II}Cl_2$(pypz-H)$(DMSO)_2$] **[1']** were added to 0.002 g (0.011 mmol) of 9S3 in 3 mL of methanol. The yellow reaction mixture was refluxed for 24 h. Then the volume was reduced and a yellow solid was obtained. The solid was washed with diethyl ether and vacuum dried. Yield: 0.022 g (42%). Anal. Found (Calc.) for $C_{14}H_{19}Cl_2N_3RuS_3$: C, 32.84 (33.24); H, 3.76 (3.89); N, 8.05 (8.37). $E_{1/2}$(CH_3CN + 0.1M TBAH): 1.16 V vs Ag/AgCl.

[Ru^{II}(pypz-H)(9S3)(DMSO)]$(PF_6)_2$ [4]. A 0.028 g (0.056 mmol) sample of [Ru^{II}Cl(pypz-H)(9S3)]Cl **[3]** and 0.011 g (0.067 mmol) of $AgNO_3$ was dissolved in 10 mL of a pre-degassed 3:1 mixture of acetone-H_2O. The mixture was refluxed in the absence of light for 4 h. After filtering the formed AgCl through a pad of Celite, 100 eq. (0.40 ml) of DMSO was added to the filtrate and the mixture was refluxed for an additional 4 h period. After precipitation of the desired complex by adding 1 mL of $NH_4PF_{6(saturated)}$ and reducing the reaction volume, the yellow solid was filtered off, washed with diethyl ether and vacuum dried. Yield: 0.014 g (30.6%). Anal. Found (Calc.) for $C_{16}H_{25}F_{12}N_3OP_2RuS_4$: C, 24.18 (24.32);

H, 3.17 (3.29); N, 5.29 (5.44). ^{1}H NMR (400 MHz, D_2O): δ = 2.70 (s, 3H, CH_3 DMSO), 2.75 (s, 3H, CH_3 DMSO), 2.77-3.35 (m, 12 H, CH_2 9S3), 7.24 (d, $^{3}J_{H,H}$ = 4 Hz, 1H, H7), 7.62 (t, $^{3}J_{H,H}$ = 8 Hz, 1H, H2), 8.08 (d, $^{3}J_{H,H}$ = 4 Hz, 1H, H8), 8.18 (t, $^{3}J_{H,H}$ = 8 Hz, 1H, H3), 8.21 (d, $^{3}J_{H,H}$ = 8 Hz, 1H, H4), 8.91 (d, $^{3}J_{H,H}$ = 8 Hz, 1H, H1) ppm. ^{13}C NMR (400 MHz, D_2O): δ = 153.3 (C5), 152.2 (C1), 140.4 (C6), 136.3 (C3), 126.8 (C8), 123.9 (C2), 105.9 (C4), 101.1 (C7), 44.3 (CH_3 DMSO), 43.0 (CH_3 DMSO), 35.4 (CH_2 9S3), 33.9 (CH_2 9S3), 32.8 (CH_2 9S3), 32.4 (CH_2 9S3), 32.1 (CH_2 9S3), 31.2 (CH_2 9S3) ppm. IR ($\nu_{max,}$ cm^{-1}): 3341, 3002, 2656, 1412, 1085, 1013, 821. E_{pa}(CH_3CN + 0.1M TBAH): 1.28 V vs Ag/AgCl. UV/Vis (H_2O, 0.1 mM) [λ_{max} nm (ε, cm^{-1} M^{1})]: 256 (13604), 294 (11124), 315 (5869), 355 (2138). ESI-MS (m/z): 507 $[M-(PF_6)_2]^{2+}$.

For the NMR assignment we have used the same numbering scheme as for the ligands displayed in *Figure 1.*

Conditions of hydration catalytic:, 0.01 mmol of the catalyst was dissolved in 3 mL of water and 1 mmol of the corresponding substrate was added. The ruthenium catalyst, water and the corresponding nitrile were introduced into a sealed tube and the reaction mixture was stirred at 80ºC for 20 hours. After this time, the nitrile was extracted with $CHCl_3$ and quantified by GC analysis. The aqueous phase was evaporated and the solid residue was dissolved in D_2O for ^{1}H-RMN analysis to identify the corresponding amide.

CHAPTER 4. RESULTS AND DISCUSSION

4.1 Synthesis

The synthetic strategies followed for the preparation of the pypz-H ligand and the Ru(II) complexes **[3]** and **[4]** is outlined in *Scheme 4* and *5*.

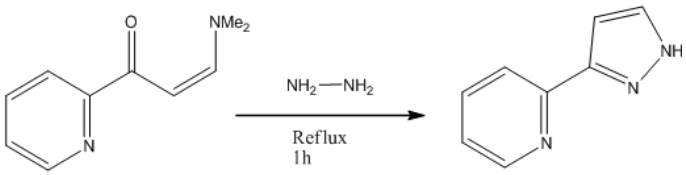

Scheme 4. Synthetic strategy to obtain the pypz-H ligand.

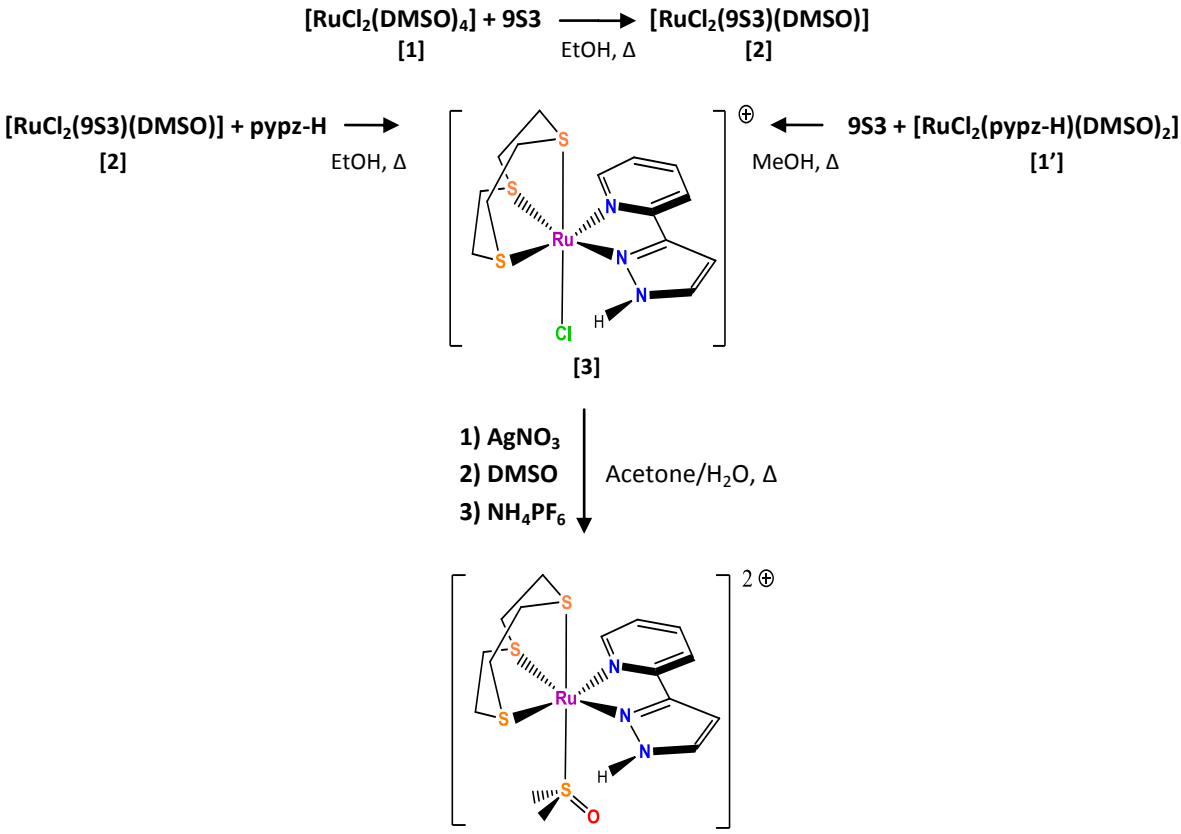

Scheme 5. Synthetic strategy and ligands used in this work.

The pypz-H ligand has been synthesized from the commercial α, β-unsaturated ketone and subsequent addition of hydrazine, after reflux during 1 h a brown precipitate was obtained corresponding to the ligand.

$[Ru^{II}Cl_2(DMSO)_4]$ **[1]** was used as starting material. The addition of 9S3 ligand to complex **[1]** produces the substitution of three DMSO ligands and the complex $[Ru^{II}Cl_2(9S3)(DMSO)]$ **[2]** was formed (see *Scheme 5*). Ruthenium complex $[Ru^{II}Cl(pypz\text{-}H)(9S3)]Cl$ **[3]** was obtained by two different synthetic strategies: I) The addition of the pypz-H ligand to complex **[2]** leads to the substitution of one DMSO and one chlorido ligands by the bidentate pypz-H ligand; II) The addition of 9S3 ligand to the complex $[Ru^{II}Cl_2(pypz\text{-}H)(DMSO)_2]$ **[1']**, previously synthesized in the group of research, leads to the substitution of two DMSO ligands and one chlorido ligand. Compound $[Ru^{II}(pypz\text{-}H)(9S3)(DMSO)](PF_6)_2$ **[4]** was obtained when DMSO is added to complex **[3]** in acetone:water solution.

4.2 Spectroscopic properties

4.2.1 IR spectroscopy

Figure 2 and *3* show the IR spectra corresponding to $[Ru^{II}Cl(pypz\text{-}H)(9S3)]Cl$ **[3]** and $[Ru^{II}(pypz\text{-}H)(9S3)(DMSO)](PF6)_2$ **[4]** respectively. The IR spectra display a band around 3350 cm^{-1} that can be assigned to the ν(NH) stretching corresponding to the pyrazolic ligands. The bands around 1420 cm^{-1} correspond to the δ (S-CH_2) deformation and the intense bands at 800 cm^{-1} corresponds to the deformation bands of N-H bonds, δ (N-H). In addition, *Figure 3* shows a band around 1090 cm^{-1} that can be assigned to the ν(SO) stretching due to the presence of the ligand DMSO. The absence of vibrations in the spectrum in the 920-930cm^{-1} range indicates a sulfur-bonded DMSO complex.

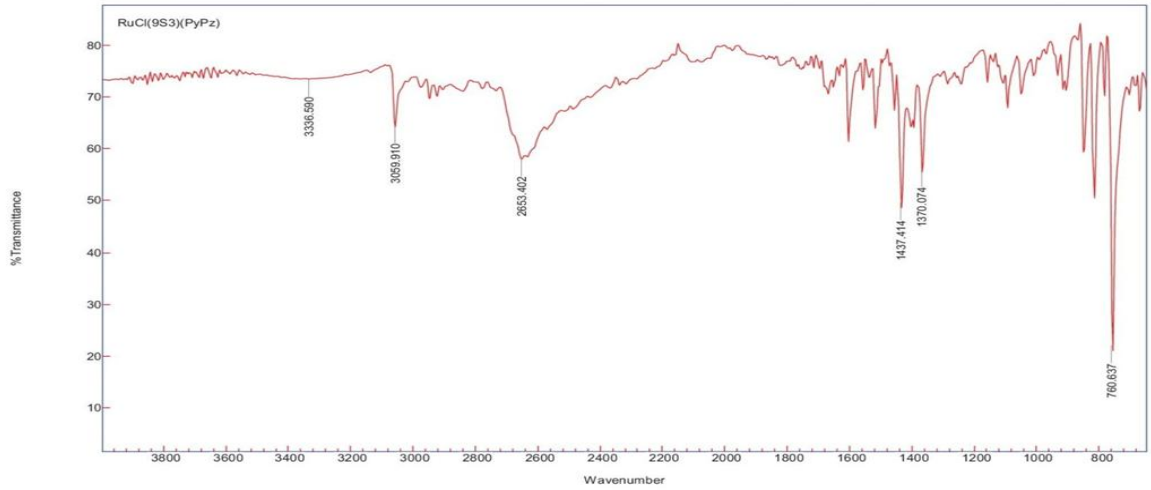

Figure 2. FTIR spectra of complex **[3]**.

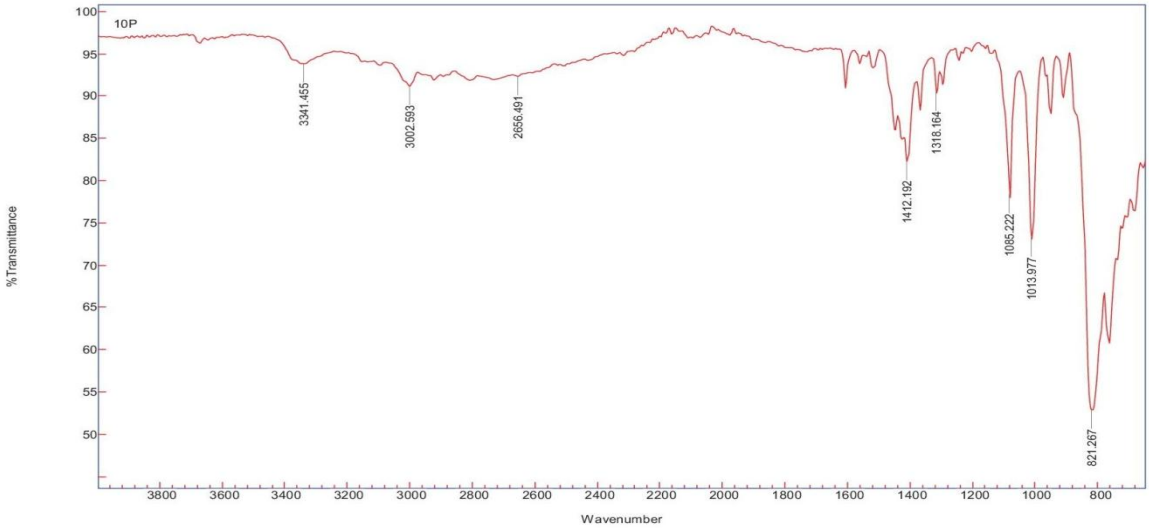

Figure 3. FTIR spectra of complex **[4]**.

4.2.2 NMR spectroscopy

The one-dimensional (1D) NMR and two-dimensional (2D) spectra of complexes **[3]** and **[4]** were recorded in methanol or deuterium oxide, respectively. *Figures 4* and *5* show the ^{1}H-NMR spectrum for complex **[3]** and **[4]**. The two complexes exhibit two sets of signals: one in the aromatic region corresponding to the pypz-H ligand and the other one in the aliphatic region assigned to the -CH_2- groups of the bonded 9S3 ligand and in the case of complex **[4]**, also to the methyl groups of the bonded DMSO ligand. The H_g of pypz-H is not observed in the ^{1}H-NMR spectra. It is worth mentioning the difference observed in the chemical shift of the two methyl groups of the ligand DMSO since they are not magnetically equivalent (see *Figure 5*).

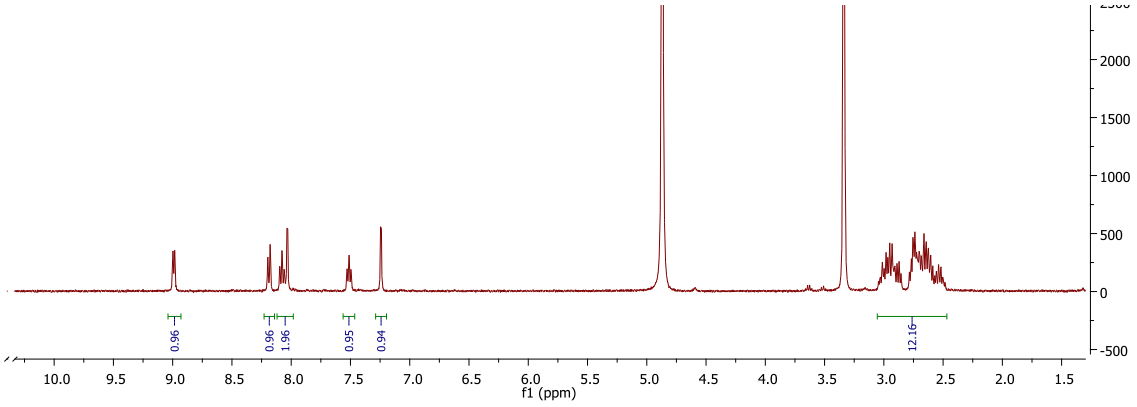

Figure 4. ^{1}H-RMN spectra of complex **[3]**.

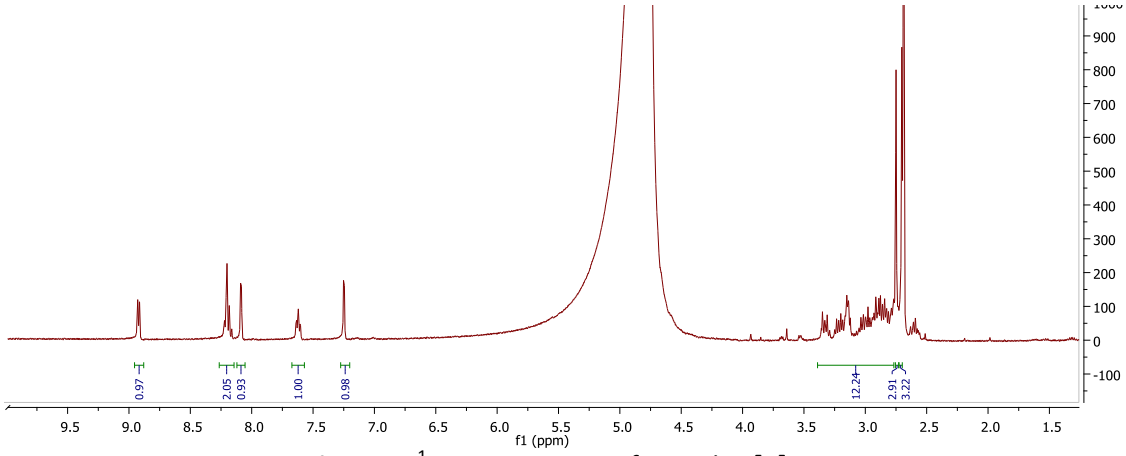

Figure 5. ^{1}H-RMN spectra of complex **[4]**.

4.2.3 UV-Vis spectroscopy

UV-Vis spectra of complex **[3]** (blue line) and **[4]** (orange line) at 0.1 mM solution of H_2O are displayed in *Figure 6*. The UV-Vis spectra for the new complexes exhibit ligand based π-π* bands below 300 nm and relatively intense bands above 300 nm mainly due to dπ-π* MLCT transitions.[38]

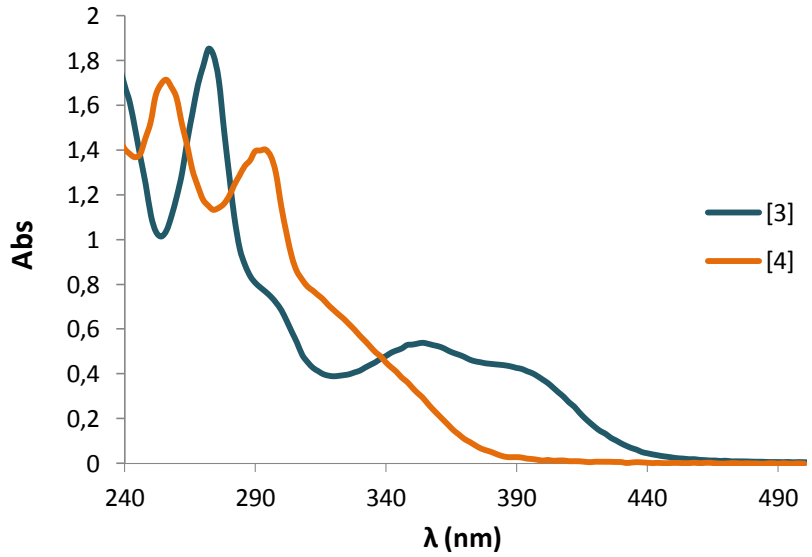

Figure 6. UV/Vis spectra of complexes **[3]** and **[4]** in H_2O.

The UV-Vis spectrum of Ru-Cl complex shows a shift of the MLCT bands to lower energy absorptions with respect to the Ru-DMSO complex, as expected from the higher σ-donor and lower π-acceptor capacity of the Ru-Cl complex that provokes a relative destabilization of the dπ(Ru) orbital.

4.3 Electrochemical properties

The redox properties of the complexes **[2]**, **[3]** and **[4]** were investigated by means of cyclic voltammetric technique (CV). The electrochemical data of complexes are presented in *Table 1* and the CV in the *Figure 7*. All cyclic voltammogram were made in CH_3CN with 0.1 M TBAH as supporting electrolyte using Ag/AgCl as reference electrode.

Table 1. Electrochemical data for complexes **[2]**, **[3]** and **[4]**.

Compound	$E_{1/2}$ (III/II) (V)	E_{pa} (V)	E_{pc} (V)
$[Ru^{II}Cl_2(9S3)(DMSO)]$ [2]	0.98	1.07	0.88
$[Ru^{II}Cl(9S3)(pypz\text{-}H)]Cl$ [3]	1.17	1.06	1.27
$[Ru^{II}(9S3)(pypz\text{-}H)(DMSO)](PF_6)_2$ [4]		1.28	

Complex **[2]** and **[3]** exhibit on-electron reversible redox wave at $E_{1/2}$=0.98 V and $E_{1/2}$=1.17 V versus Ag/AgCl, respectively. On the other hand, complex **[4]** shows a chemically irreversible wave with E_{pa}=1.28 V. Comparing the redox potential of complexes **[2]** and **[3]**, the substitution of one DMSO and one chlorido ligand by the pyridine pyrazole ligand leads to an increase in the redox potential (0.98 V for **[2]** vs 1.17 V for **[3]**) this fact point out the higher π-acceptor capacity of the pypz-H ligand with regard to the presence of the two monodentate ligands, Cl and DMSO. In the case of complexes **[3]** and **[4]**, the substitution of one chlorido by one DMSO ligand leads to the increase of potential due to the higher π-acceptor capacity of the DMSO ligand by report to chlorido and we have also observed that the CV of complex **[4]** becomes irreversible.

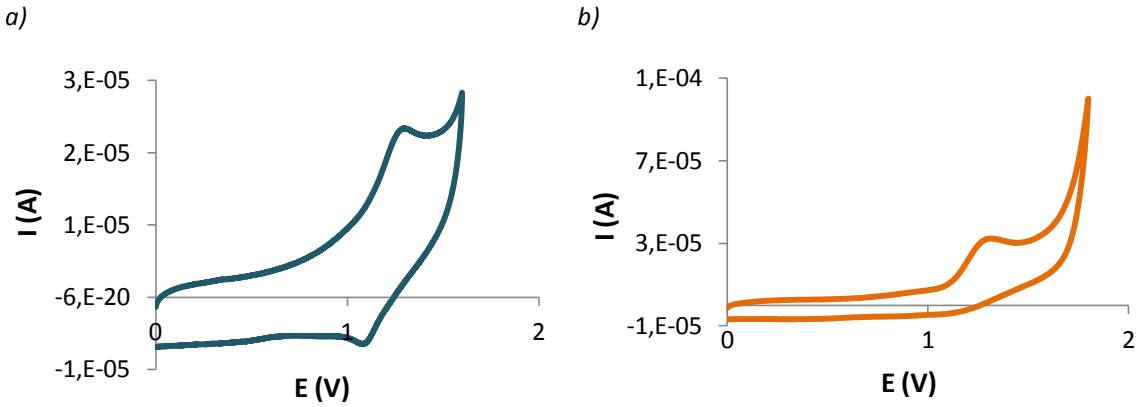

Figure 7. Voltammogram in CH_3CN solution: **a** for complex **[3]** and **b** for complex **[4]**.

4.3.1 Chemical behavior in aqueous solution

In order to obtain more information about the lability of the chlorido and DMSO ligands in the synthesized complexes, given their potential involvement in some catalytic processes, we have studied the behavior of our compounds in aqua medium.

The reactions attributed to the substitution of chlorido and DMSO ligands by aqua ligand are the ones following:

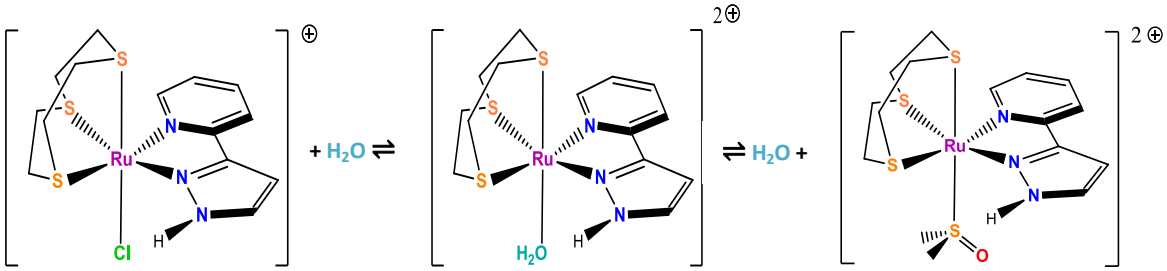

Shame 6. Aquations for both complexes **[3]** and **[4]**.

0.1 mM solution of complexes **[3]** and **[4]**, in water have been monitored through UV-Vis experiments. The chlorido ligand in the compound **[3]** turned out to be very labile in aqueous solution. Immediately after dissolution in water at room temperature, conversion of the initial chlorido complex into the corresponding aqua specie was observed. *Figure 8* show a shift of the MLCT bands of complex **[3]** to higher energy absorptions and four isosbestic points at 275, 280, 355 and 375 nm can be observed, confirming the substitution of a chlorido ligand by a high π-acceptor aqua ligand and the formation to a new compound that presumably corresponds to $[Ru^{II}(pypz\text{-}H)(OH_2)(9S3]^{2+}$ complex **[5]**.

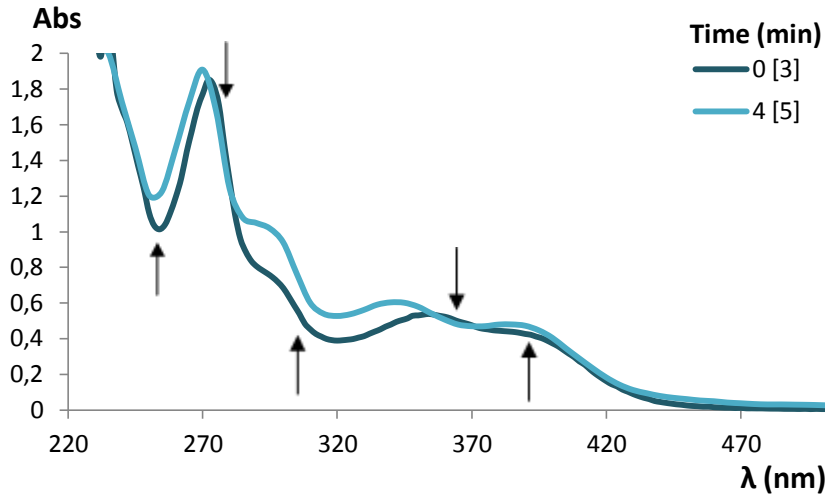

Figure 8. Evolution of an aqueous solution of complex **[3]** at room temperature.

Contrary to the observed for the chlorido complex, the UV-Vis spectrum of complex **[4]** not shows any significant changes at room temperature during 24 hours. However, the UV-Vis spectra of complex **[4]** registered in water at 70 ºC during 180 minutes (see *Figure 9*) show four isosbestic points at 243, 262, 281 and 336 nm and a shift of the MLCT bands to lower energy confirms the net conversion to the similar complex **[5]** described previously.

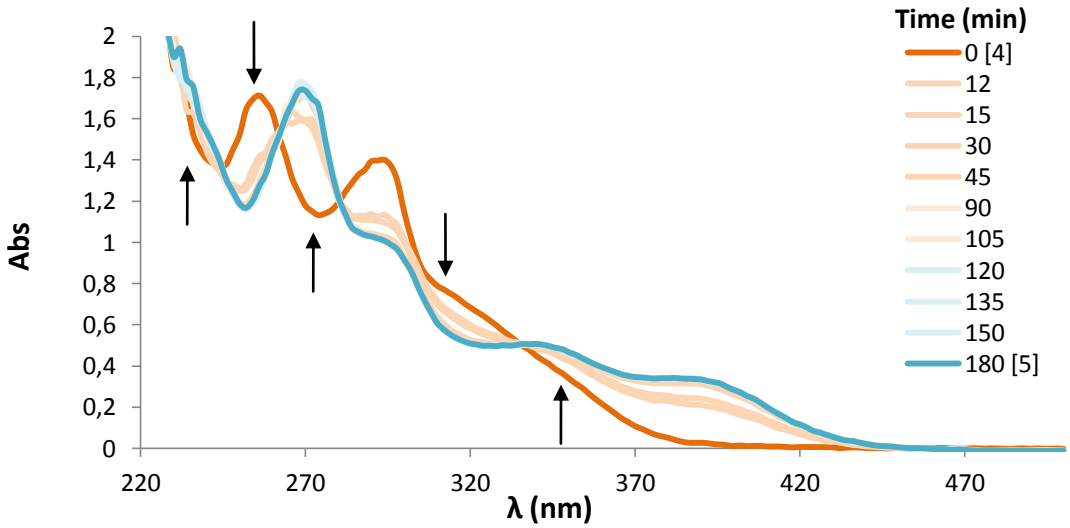

Figure 9. Evolution of an aqueous solution of complex **[4]** by warming at 343 K for 3 h.

4.3.2 Kinetics of Aquation

As we have evidenced the time-dependent changes in the UV-Vis with the isosbestic points we can suggest the occurrence of a hydrolytic process. Thus, the kinetics of aquation of compound **[3]** and **[4]** was quantitatively studied on 0.1mM solution by UV/Visible spectroscopy, at room temperature for **[3]** and 70°C for **[4]**.

256nm for complex **[3]** and 274 nm for complex **[4]** were the wavelength selected for the kinetic studies. The time dependence of the absorbance followed a first order kinetics in both cases and the analyses of the dates let to obtain the rate constant k_{H2O}. We show the study corresponding to the kinetics of aquation of complex **[4]** (see *Figure 10*). Similar behavior had been observed for complex **[3]**.

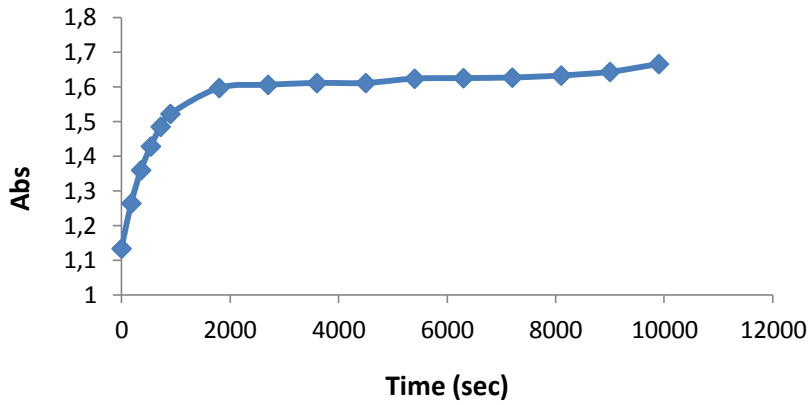

Figure 10. Time-dependence of the absorbance during the aquation of complex **[4]** in water (λ=274 nm).

The method of obtaining the first-order rate constant is presented below. The kinetic study to determine K_{H2O} relies on the *Beer-Lambert* law.

$$A = \varepsilon \cdot c \cdot l \qquad (3)$$

Where,
A = absorbance
l = dimension of the cuvette (cm)
c = concentration of solution (mol dm^{-3})
ε = molar extinction

Considering a first kinetic reaction and according to the Beer-Lambert Law, the absorbance is proportional to the concentration of the complex in solution, we obtain:

$$ln(A_{bst} - Abs_{\infty}) = ln(Abs_0 - A_{bs\infty})] - k_{obs}t \qquad (4)$$

A plot of ln(A-A∞) versus time yields the rate constant K_{H2O} (see *Figure 11*) for complex **[4]**. *Table 2* shows the rate constant K_{H2O} for complex **[3]** together with other rate constants described in the literature for purposes of comparison.

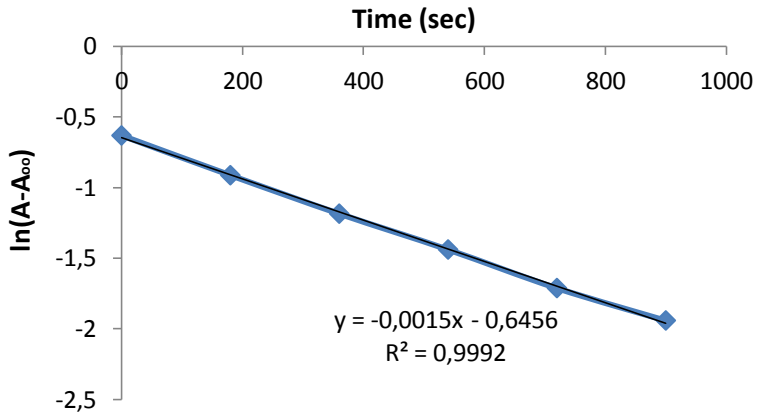

Figure 11. Time-dependence of the ln(A-A∞) during the aquation of complex **[4]** (at 274 nm, 0.1 mM).

Table 2. Rate constants for the aquation of complexes **[3]** and **[4]** and two new compounds described in the literature.

Compound	K_{obs} (s^{-1})	T (°C)
$[Ru^{II}Cl(pypz\text{-}H)(9S3)]Cl$ [3]	$16.9 \cdot 10^{-3}$	25
$[Ru^{II}(pypz\text{-}H)(9S3)(DMSO)](PF_6)_2$ [4]	$1.5 \cdot 10^{-3}$	70
$[Ru^{II}Cl(ppt)(9S3)][CF_3SO_3]$ [6]	$4.10 \cdot 10^{-5}$	25
$[Ru^{II}Cl(Cl\text{-}tpy)(dach)]Cl$ [7]	$3.94 \cdot 10^{-3}$	25

[6]: ptt, 1-(2-picolyl)-4-phenyl-1H-1,2,3-triazole. **[7]**: Cl-tpy, 4-chloro-2,2';6',2''-terpyridine; dach, 1,2-diaminocyclohexane.

As we can see in *Table 2*, complex **[3]** hydrolyzes faster than the complex **[4]**, contrary to chloride complex the DMSO derivative is more stable in aqueous solution. It is worth noting that the aquation rate of the chlorido complex **[3]** is 100-fold faster than the compound **[6]**[15] which presents a similar structure but a different bidentate ligand and 4–fold faster than complex **[7]**[39], containing a terpyridine as tridentate ligand and an aliphatic diamine as bidentate ligand.

This latter presents an important anticancer activity; in this context, compound **[3]** could be used as a potential antitumor agent due to the good solubility in water, together with the easy release of Cl ligand to form the aqua complex.

4.3.3. Redox properties of Ru-aqua complex

We had above studied the kinetics properties of the aqua complex **[5]** obtained in the substitution process. The redox properties of Ru-aqua complex are pH dependent because of the capacity of the aqua ligand to lose protons upon oxidation of the complex, which also makes the high oxidation states easily accessible. This pH-dependent behavior is manifested in DPV experiments performed at different pH values (see *Figure 12)*.

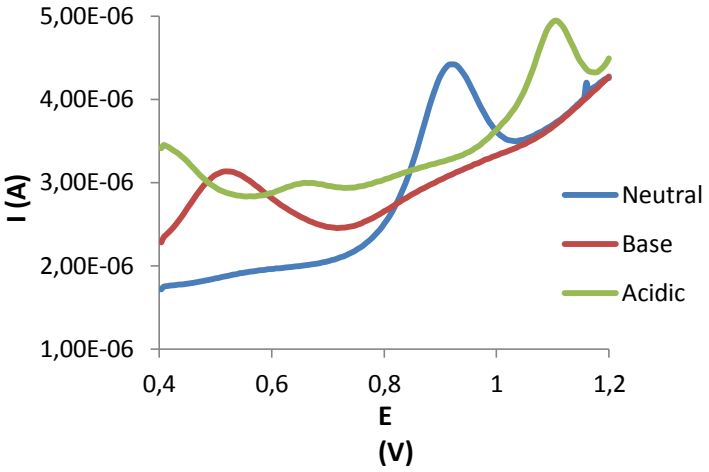

Figure 12. Differential pulse voltammetries of complex **[5]** in water at pH=2.6 (green), 6.7 (blue) and 8.8 (red).

Figure 13 shows the Pourbaix diagram which plot $E_{1/2}$ versus pH, where different species can be observed at pH> 2.

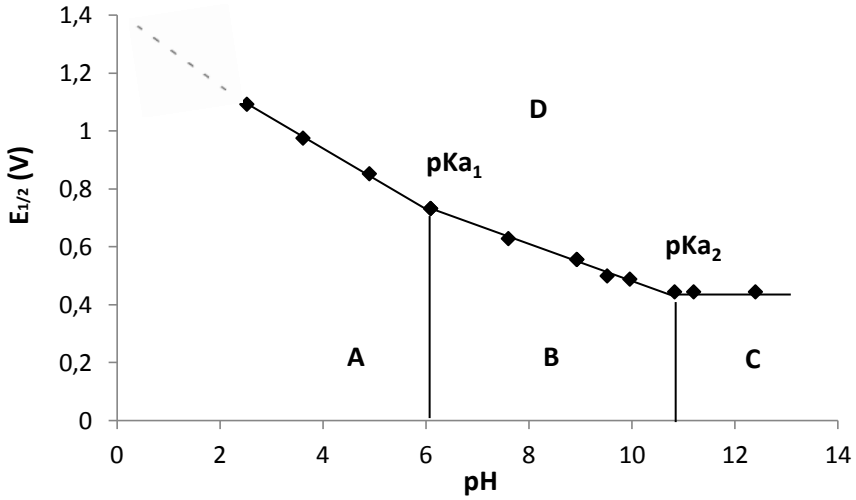

Figure 13. Pourbaix diagram of aqua complex **[5]**, being A, B, C and D the species shown in equations 5, 6 and 7.

Within the pH range 2-6.1 approximately, the couple Ru(III/II) decrease 100 mV for pH unit. This variation according to the Nernst prediction (*Equation 1*) is consistent with a process that exchanged two protons and one electron, with a theoretical slope of 118 mV for pH unit.

$$\mathbf{[Ru^{II}(pypz\text{-}H)(OH_2)(9S3)]^{2+}\ (A)} \rightleftharpoons \mathbf{[Ru^{III}(pypz)(OH)(9S3)]^{+}\ (D) + 2H^{+} + e^{-}} \quad (5)$$

Within the pH range 6.1-10.8, the couple Ru(III/II) decrease 62 mV for pH unit. This value is near to the value of Nernst prediction of 59 mV for pH unit. Where one proton and one electron are exchanged as you can see in the equation following (see *Equation 6)*:

$$\mathbf{[Ru^{II}(pypz)(OH_2)(9S3)]^{+}\ (B)} \rightleftharpoons \mathbf{[Ru^{III}(pypz)(OH)(9S3)]^{+}\ (D) + 1H^{+} + e^{-}} \quad (6)$$

Under strong basic conditions, pH >10.8, the wave potential is not dependent from de pH and the process can be represented according to the *Equation 7*:

$$\mathbf{[Ru^{II}(pypz)(OH)(9S3)]^{2+}\ (C)} \rightleftharpoons \mathbf{[Ru^{III}(pypz)(OH)(9S3)]^{+}\ (D) + e^{-}} \quad (7)$$

The changes in the slope correspond to the pKa values of the Ru(II) species and are indicated by vertical lines in each case, being for complex **[5]** $pKa_1 = 6.1$ and $pKa_2 = 10.8$, respectively.

$$\mathbf{[Ru^{II}(pypz\text{-}H)(OH_2)(9S3)]^{2+}\ (A)} \overset{pKa_1}{\rightleftharpoons} \mathbf{[Ru^{II}(pypz)(OH_2)(9S3)]^{+}\ (B) + 1H^{+}} \quad (8)$$

$$\mathbf{[Ru^{II}(pypz)(OH_2)(9S3)]^{+}\ (B)} \overset{pKa_2}{\rightleftharpoons} \mathbf{[Ru^{II}(pypz)(OH)(9S3)]^{2+}\ (C) + 1H^{+}} \quad (9)$$

The pKa values are displayed in *Table 3* along with other ruthenium complex containing a pyrazole based ligand as bidentate ligand for purposes of comparison.[40]

Table 3. p*K*a values for aqua complexes **[5]** and **[8]**.

Compound	pKa_1	pKa_2
$[Ru^{II}(pypz\text{-}H)(OH_2)(9S3)]^{2+}$ **[5]**	6.1	10.8
$[Ru^{II}(bpp)(tpy)(OH_2)]^{+}$ **[8]**	6.9	11.1

[8]: bpp, bis(2-pyridyl)pyrazole; tpy, 2,2';6',2''-terpyridine.

It can be observed that complex **[5]** display lower pKa values than the corresponding complex **[8]** (6.1 and 10.8 vs. 6.9 and 11.1). This higher acidic character for complex **[5]** is in accordance with the enhanced electron-withdrawing nature of the 9S3 ligand when compared to the tpy ligand.

4.4 Catalytic hydration of nitriles

We have checked the previously reported complexes $[Ru^{II}Cl_2(9S3)(DMSO)]$ **[2]**, $[Ru^{II}Cl(pypz\text{-}H)(9S3)]Cl$ **[3]** and $[Ru^{II}(pypz\text{-}H)(9S3)(DMSO)](PF_6)_2$ **[4]** in the hydration of different nitriles using water as a solvent at 80ºC. Conversion and selectivity values are summarized in *Table 4* together with the conditions used in the catalysis. The remaining substrate has been quantified through GC chromatography with biphenyl as the internal standard and the hydrolysis products have been analyzed by NMR spectroscopy and compared to pure samples of the corresponding amide and acid derivates.

Table 4. Ru-catalyzed hydration of nitriles to amides in water using complexes **[2]**, **[3]** and **[4]** as catalysts. Selectivity and conversion are given in %.

Complex	**[2]**		**[3]**		**[4]**	
Substrate	**Conv.**	**Sel.**	**Conv.**	**Sel.**	**Conv.**	**Sel.**
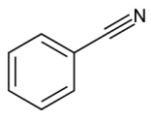 Benzonitrile	24.6	> 98	45.4	> 98	69.4	> 98
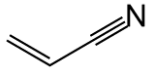 Acrylonitrile	26.9	>98	23.1	>98	64.4	>98

Reactions performed at 80ºC using 1 mmol of nitrile in 3 ml of water. [Substrate]:[Ru] = 100 : 1. Time: 20 h. Selectivity = (amide yield/substrate conversion) x 100.

As can be observed in *Table 4*, all complexes were found to be active towards nitrile hydration despite obtaining from moderate to high conversion values, being complex **[4]** the one which show highest conversion values for the three substrates proved. In all cases, high selectivity values were obtained.

The general mechanism currently accepted in the hydration of nitriles begins with a substitution process, where a ligand is replaced by the corresponding nitrile in the metal coordination environment and a subsequent nucleophilic attack of water to the nitrile carbon atom takes place (*section 1.4.2*). The electronic characteristics of the ligands in the catalyst influence the ability of the metal to activate the nitrile substrate: a high electron-withdrawing character of the ligands will drive the metal to a stronger activation of the coordinated nitrile substrate, making it more susceptible to a water nucleophilic attack. Regarding the hydration of benzonitrile we can observed that conversion values obtained with complexes **[3]** and **[4]** containing both the pyrazolic ligand are higher than the values obtained using complex **[2]** as catalytst, where only monodentate ligands chlorido and DMSO are present together whit the 9S3 ligand; this fact point out the importance of the bidentate pyridine pyrazole ligand in the catalytic process. This behavior is not observed for the acrylonitrile substract where complex **[3]** shows lower values compared with complex **[4]**.

The results are in agreement with the accepted mechanism described above since complex **[4]**, with the π-acceptor DMSO and pypz-H ligands is the one displaying the higher conversions for all the substrates tested. Ligands that favour the removal of electron density from the Ru(II) metal centre in turn also reduce the electron density in the C≡N bond of the bonded nitrile ligand and, therefore, enhance the electrophilicity of the C atom where the OH^- attacks. There is a direct relationship between the Ru(III/II) reduction potentials and the conversion values (complex **[4]** presents a Ru(III/II) redox potential around 0.1 V higher than complex **[3]** and 0.3 V than complex **[2]**). The electronic properties of the substrates also influence the extent of the hydration reaction where lower performance values are observed for acrylonitrile as a substrate with less activating effect that benzonitrile.

CHAPTER 5. CONLCUSIONS

The main conclusions drawn from this research work are listed below:

- I have learnt the techniques of synthesis and spectroscopic and electrochemical characterization characteristic of a research laboratory.

- The ligand pypz-H and the complexes [Ru^{II}Cl(pypz-H)(9S3)]Cl **[3]** and [Ru^{II}(pypz-H)(9S3)(DMSO)][$(PF_6)_2$] **[4]** have been synthesized and characterized by spectroscopic and electrochemical techniques.

- Electrochemical experiments via CV point out the electronic characteristics of the ligands, showing lower redox potentials for complex **[3]** than complex **[4]** as expected from the higher σ-donor capacity of the chlorido versus DMSO ligand.

- The complexes studied are well soluble in water and the study of the chemical behaviour in aqueous solution of these complexes let to the formation of the aqua complex that presumably corresponds to $[Ru(pypz\text{-}H)(OH_2)(9S3)]^{2+}$ **[5]**. Aquation rate constants point out that complex **[3]** releases the chlorido ligand at much faster rate than complex **[4]** which is inert a room temperature (do not release the monodentate ligand). In the case of complex **[3]** the equilibrium was reached ca. 4 minutes after dissolution. For complex **[4]** the substitution of DMSO by aqua ligand takes place to high temperature (70°C) and was reached ca. 180 minutes after dissolution.

- The redox characterization of the Ru-aqua complex **[5]** through a Pourbaix diagram showed the occurrence of one-electron Ru(III/II) redox processes in the range of pH studied. The pKa values have been also calculated, being 6.1 for pKa_1 and 10.8 for pKa_2.

- Compounds **[2]**, **[3]** and **[4]** were checked in the hydration of nitriles in water at 80°C, showing moderate to high conversion values and in all cases high selectivity values for the corresponding amides. Complex **[4]** shown the best conversion values in accordance with the electronic properties of the ligands in the complex.

CHAPTER 6. BILBIOGRAPHY

[1] Qu, P.; Thompson, D. W.; Meyer, G. J. *Langmui,* **2000**, *16*, 4662.

[2] Murahashi, S.I.; Takaya, H.; Naota, T. *Pure Appl. Chem.* **2002**, *74*, 19. Rodríguez M.; Romero, I.; Llobet, A.; Deronzier, A.; Biner, M.; Parella, T.; StoeckliEvans H. *Inorg. Chem*. **2001**, *40*, 4150.

[3] Nikolau, S.; Toma, H.E. *J. Chem. Soc., Dalton Trans.* **2002**, 352. Rodríguez, M.; Romero, I.; Llobet, A.; Collomb-Dunand-Sauthier, M. N.; Deronzier, A.; Parella, T.; Stoeckli-Evans, H. *J. Chem. Soc., Dalton Trans.* **2000**, 1689.

[4] Clarke, M. J. *Coord. Chem. Rev.* **2003**, *236*, 209.

[5] Balzani, V.; Bergamini, G.; Marchioni, F.; Ceroni, P. *Coord. Chem. Rev*. **2006**, *250*, 1254.

[6] Zhang, S.; Ding, Y.; Wei, H. *Molecules.* **2014**, *19*, 11933.

[7] Coe, B. J. *Coord. Chem. Rev*. **2013**, *257*, 1438. Yoshida, J.; Watanabe, G.; Kakizawa, K.; Kawabata, Y.; Yuge, H. *Inorg. Chem*. **2014**, *52*, 11042.

[8] Silva, D. D. O. *Anticancer Agents Med. Chem*. **2010**, *10*, 312.

[9] Alstreen-Acebedo, J. H.; Brennaman, M.K.; Meyer T.U. *Inorg. Chem.* **2005**, *44*, 6802-6872. Hammarstrom, L.; Sun, L.C.; Akermark, B.; Stryring, S. *Catal. Today*. **2000**, *58*, 57-69.

[10] Barigelletti, F.; Flamigni, L. *Chem. Soc. Rev.* **2000**, *29*, 1. Yin, J.-F.; Velayudham, M.; Bhattacharya, D.; Lin, H.-C.; Lu, K.-L. *Coord. Chem. Rev*. **2012**, *256*, 3008.

[11] Jiang, C.W.; Chao, H.; Hong, X. L.; Li, H.; Mei, W. J.; Ji, L. N. *Inorg. Chem. Commun.* **2003**, *6*, 773-775.

[12] Alessio, E.; Mestroni, G.; Nardin, G.; Attia, W. M.; Calligaris, M.; Sava, G.; Zorzet, S. *Inorg. Chem.* **1988**, *27*, 4099.

[13] Martínez, R.; Ramón, D. J.; Yus, M. *Eur. J. Org. Chem.* **2007**, 1599.

[14] Bratsos, I.; Simonin, C.; Zangranado, E.; Gianferrara, T.; Bergamo, A; Alessio, E. *Dalton Trans.* **2011**, *40*, 9533.

[15] Bratsos, I.; Urankar, D.; Zangrando, E.; Genova-Kalou, P.; Kosmrlj, J.; Alessio, E.; Turel, I. *Dalton Trans.* **2011**, *40*, 5188-5199.

[16] Iengo, E.; Zangrando, E.; Baiutti, E.; Munini, F.; Alessio, E. *Eur. J. Inorg. Chem.* **2005**, 1019-1031.

[17] Cotton, F. A.; Elder, R. C. *J. An. Chem. Soc.* **1960**, *82*, 2986. Meek, D. W.; Straub, D. K.; Drago, R. S. *Bull. Chem. Soc. Japan* **1960**, *33*, 861.

[18] Baranoff, E.; Collin, J. P.; Furusho, J.; Furusho, Y.; Laemmel, A. C.; Sauvage, J. P. *Inorg. Chem.* **2002**, *41*, 1215.

[19] Alessio, E.; Mestroni, G.; Bergamo, A.; Sava, G. *Curr. Top. Med. Chem.* **2004**, *4*, 1525.

[20] Smith, M. K.; Gibson, J. A.; Young, C. G.; Broomhead, J. A.; Junk, P. C.; Keene, F. R. *Eur. J. Inorg. Chem.* **2000**, 1365.

[21] Evans, I. P.; Spencer, A.; Wilkinson, G. *J. Chem. Soc. Dalton Trans*. **1973**, *2*, 204.

[22] Khan, M. T.; Mohiuddin, R.; Vancheesan, S.; Swamy, B. *Ind. J. Chem. Section A: Inorg., Phys., Theor.& Anal.* **1981**, *20A*, 564.

[23] Gonsalvi, L.; Arends, I. W. C. E.; Sheldon, R. A. *Chem. Commun.* **2002**, *3*, 202.

[24] Van der Drift, R. C; Sprengers, J. W.; Bouwman, E.; Mul, W. P.; Kooijman, H.; Spek, A. L.; Drent, E. *Eur. J. Inorg. Chem.* **2002**, *8*, 2147.

[25] Costentin, C.; Robert, M.; Saveant, J.-M. *Chem. Rev.* **2010**, *110*, PR1-PR40.

[26] Yamada, H.; Kobayashi, M. *Biosci. Biotechnol. Biochem*. **1996**, *60*, 1391.

[27] Moorthy, J. N.; Singhal, N. *J. Org. Chem*. **2005**, *70*, 1926. Kornblum, N.; Singaram, S. *J. Org. Chem*. **1976**, *44*, 4727.

[28] Valeur, E.; Bradley, M. *Chem. Soc. Rev.* **2009**, *38*, 606.

[29] Diamond, S. E.; Grant, B.; Tom, G. M.; Taube, H. *Tetrahedron Lett.* **1974**, *15*, 4025.

[30] Murahashi, S. I.; Sasao, S.; Saito, E.; Naota, T. *Tetrahedron,* **1993**, *49*, 8805. Murahashi, S. I.; Naota, T. *Bull. Chem. Soc. Jpn.* **1996**, *69*, 1805. Murahashi, S. I.; Takaya, H. *Acc. Chem. Res*. **2000**, *33*, 225.

[31] Murahashi, S. I.; Naota, T. *Bull. Chem. Soc. Jpn.* **1996**, *69*, 1805.

[32] Murahashi, S. I.; Sasao, S.; Saito, E.; Naota, T. *J. Org. Chem*. **1992**, *57*, 2521.

[33] Parkins, A. W. *Platinum Met. Rev.* **1996**, *40*, 169.

[34] Alagesan, M.; Bhuvanesh, N. S. P.; Dharmaraj, N. *Dalton Trans.* **2014**, *43*, 6087.

[35] Smith, M. K.; Gibson, J. A.; Young, C. G.; Broomhead, J. A.; Junk, P. C.; Keene, F. R. *Eur. J. Inorg. Chem.* **2000**, 1365.

[36] Ferrer, I.; Rich, J.; Fontrodona, X.; Rodríguez, M.; Romero, I. *Dalton Trans.* **2013**, *42*, 13461-13469.

[37] Brunner, H.; Scheck, T. *Chem. Ber*. **1992**, *125*, 701.

[38] Balzani, V.; Juris, A.; Veturi, M. *Chem. Rev*. **1996**, *96*, 759.

[39] Rilak, A.; Bratsos, I.; Zangrando, E.; Kljun, J.; Turel, I.; Bugarcic, Z.; Alessio, E. *Inorg. Chem.* **2014**, *53*, 6113-6126.

[40] Sens Llorca, C. *Síntesi i caracterització de nous complexos mononuclears de ruteni amb el lligand dinucleant 3,5-bis(2-piridil)pirazola.* Universitat de Girona, 2002.